

## Linear response to spin-dependent and spin-independent fields of alkali metal clusters

This article has been downloaded from IOPscience. Please scroll down to see the full text article.

2000 J. Phys.: Condens. Matter 12 4365

(<http://iopscience.iop.org/0953-8984/12/19/307>)

View [the table of contents for this issue](#), or go to the [journal homepage](#) for more

Download details:

IP Address: 171.66.16.221

The article was downloaded on 16/05/2010 at 04:53

Please note that [terms and conditions apply](#).

## Linear response to spin-dependent and spin-independent fields of alkali metal clusters

M B Torres<sup>†</sup> and L C Balbás<sup>‡</sup>

<sup>†</sup> Departamento de Matemáticas y Computación, Universidad de Burgos, 09006 Burgos, Spain

<sup>‡</sup> Departamento de Física Teórica, Universidad de Valladolid, 47011 Valladolid, Spain

Received 28 January 2000

**Abstract.** We have obtained the dipole response functions of alkali-metal clusters to spin-dependent and spin-independent fields within the framework of the time-dependent local-spin-density approximation. As test cases we have studied the response of spherical jellium clusters with spin-saturated configurations ( $\text{Na}_9^+$ ,  $\text{Na}_8$  and  $\text{Na}_{20}$ ) and with fully spin-polarized configurations (the spherical isomer of  $\text{Na}_6^+$  and  $\text{Na}_{13}$ ). For a spin-dependent excitation we have obtained in all these clusters a strongly collective spin mode of surface type lying at lower energies than the unperturbed particle–hole excitations. This mode uncouples cleanly from the electric dipole mode (Mie plasmon) in the case of spin-saturated clusters, but if the ground state breaks spin symmetry by a finite spin polarization the two modes turn out to be intertwined in the responses to spin-dependent as well as spin-independent fields.

### 1. Introduction

Much effort has been devoted in the last years to study the excitations induced in metal clusters, cavities and shells by external probes: for reviews see [1, 2]. Up to now only the dipole surface Mie plasmon, lying at energies considerably higher than the original particle–hole (p–h) excitations and carrying a large fraction of the energy weighted sum rule, has been experimentally observed in photoabsorption experiments [3]. This resonance, which appears as an ideally harmonic mode, has been in some cases an important tool to gather information about the structural properties of clusters [4].

A theoretical description of plasmon states in metal clusters has been worked out by means of the density–density response function obtained within the framework of the time-dependent local-density approximation (TDLDA) [5]. This approach, which is based on the mean field density functional theory, within the local-density approximation for treating the electron–electron interaction, has been extensively applied in the past to simple metal clusters using the jellium model to describe the positively charged background (for a review see [2]). The corresponding solutions can be worked out either in coordinate space [6] or in configuration space [7]. In both cases this is done in a basis that is built up of p–h excitations involving the single particle orbitals where the electrons move. Although the structureless jellium model can qualitatively explain most of the observed gross features of the photoabsorption spectra of alkali clusters in the optical region, it is possible, nowadays, to use ionic pseudopotentials with different sophistication to describe the ionic part of the Hamiltonian, when finesse is needed [4, 8, 9]. The accuracy of the TDLDA within non-local pseudopotential calculations has been well stabilized recently [10]. Recent calculations using local ionic pseudopotentials are reported in [8, 11, 12].

Apart from electric dipole modes in the optical region, other excitation channels of finite systems are much harder to access experimentally and they have been much less studied. The fast development of experimental techniques and in particular the utilization of electrons as probes authorizes us however to expect in the near future the observation of other modes of excitation in finite systems and in particular of spin dipole modes, which play a role in bulk matter [13]. This is what happened in the study of excitations of the atomic nucleus where currently a wide experimental study of spin modes is available [14]. Due to the similarity between metal clusters and nuclei, many models of nuclear theory have been applied to the study of metal clusters. On the other hand, with the present experimental resolution, the spin-orbital interaction in metal clusters is negligible and thus spin and orbital collective modes are well uncoupled. The separation of these two modes in clusters is easier than in nuclei.

The existence of spin modes deserves a detailed study in metal clusters, with  $N$  electrons, where the search for low-energy excitations has been a central subject in the exploration of their collective properties. In contrast to the plasmon, these resonances are expected to be strongly Landau damped in the infinite system because they have excitation energies lying within the continuum of single p-h excitations. Some years ago it was however pointed out that in finite systems the situation could be different due to the shell structure effects. Multipole resonances of spin character caused by the external field

$$V_{ext}^{\sigma} = \sum_{j=1}^N r_j^L Y_{L0} \sigma_j^z \quad (1)$$

( $r$  and  $\sigma^z$  are the radial position and the third component of the spin vector, respectively) have been studied within the sum rule approach (SRA) [15] and the random phase approximation (RPA) [16, 17] in metal clusters, showing that the shell structure is responsible for the occurrence of a spin collective mode at lower energy than typical unperturbed p-h transitions. For the dipole case,  $L = 1$ , the operator  $V_{ext}^{\sigma} \approx \sum_{j=1}^N z_j \sigma_j^z$  provides the opposite shifts of spin-up and spin-down electrons in the  $z$ -direction, where  $z$  is the third component of the position vector.

Unlike the electric resonances, the residual interaction for spin resonances is defined only by the exchange and correlation (xc) term, since only the xc term depends on the spin density (see below, section 2). Therefore the study of spin resonance modes can provide valuable information about xc effects in clusters.

Lipparini and Califano [15] have also calculated the collective resonance frequencies in metal spheres in a simple way in the framework of the hydrodynamic model, comparing the results with the ones of the SRA. On the other hand, Serra and co-workers [16] have calculated in coordinate space and within the TDLDA the spin excitations of closed-shell alkali-metal clusters to an external multipole spin-dependent field. They have predicted the existence of a strongly collective spin mode of surface type appearing at much lower energy (below 1.5 eV) than the Mie plasmon and they have discussed its evolution with size. Mornas and co-workers [17] have also studied the spin modes of selected sodium clusters, including the strongly spin-polarized  $\text{Na}_6^+$  cluster, using an extension of the RPA technique which allows the exploration of various deformations [18]. The same technique has been applied recently [12] to the triaxial cluster,  $\text{Na}_{12}$ .

The linear response theory to an external field with an uniform direction of magnetization, as in equation (1), was derived by Williams and Von Barth [19] and firstly applied to unpolarized sodium clusters by Serra and co-workers [16]. In this paper we extend somewhat the formulation of the TDLSDA given in [19] which will allow us to study the response of spin-saturated clusters as well as strongly spin-polarized clusters to spin-dependent and spin-independent fields [20]. In this way we simulate the effect on the electronic spins of an

appropriate external probe such as a photon or an electron beam. The coupling of this external probe with the orbital angular momentum of the electrons, leading to orbital magnetism [21] is not considered.

It has been shown [12] that the spin modes suffer a spectral fragmentation which is a consequence of the symmetry breaking due to the underlying ionic structure, as in the case of dipole plasmon modes [4, 5]. Our purpose is to investigate how the spin degree of freedom of metal clusters affects their response properties to external spin-dependent and spin-independent fields. To this end we perform TDLSDA calculations restricted, for the sake of simplicity, to spherical symmetry. This restriction, of course, reduces the space of accessible excitations. However, the fact to compare the induced spin-density modes with the total density modes using the spherical restriction in both cases allow us to obtain clear hints on the effect of the spin degree of freedom. Thus, we can analyse the possible cross talk between the two types of excitation without bothering about additional mode mixing through deformation.

In section 2 the TDLSDA formalism is developed in a general way. In section 3 we present and discuss our results for the spin-saturated clusters  $\text{Na}_9^+$ ,  $\text{Na}_8$  and  $\text{Na}_{20}$  as well as the strongly spin-polarized clusters, the spherical isomer of  $\text{Na}_6^+$  and  $\text{Na}_{13}$ . General conclusions and future prospects are collected in section 4.

## 2. Theoretical model

The calculation of linear response functions of inhomogeneous many-electron systems within density-functional theory is an interesting and useful area of research because this theory currently seems to offer the only practical way in which to incorporate the effects of exchange and correlation. That theory is usually designed to be exact in the limit of a slowly varying density and will therefore give a response function with the correct long-wavelength limit.

By means of density-functional theory we can, in principle, calculate the spin-density matrix  $n^{\sigma\sigma'}(\mathbf{r})$  of the ground state of any electronic system subject to a local spin dependent external potential  $w^{\sigma\sigma'}(\mathbf{r})$ , which describes the coupling of the charge and spin of electrons to the external field. In practice we must construct some approximation for the functional dependence of the total energy on the density matrix  $n^{\sigma\sigma'}(\mathbf{r})$  and we can obtain the ground state energy and the density matrix from a relatively simple method based on an equivalent one-electron formulation. Density-functional theory can also be used to obtain different time-dependent correlation functions such as the density–density response function needed for optical absorption [5, 6] or the spin–spin response function giving information on the spin excitations [19]. This is due to the fact that the Hamiltonian, and therefore all expectation values with respect to its eigenvectors, are functionals of the density matrix.

In order to demonstrate the basic ideas, we will here consider the case of a uniform direction of magnetization. The density matrix of a system with  $N$  electrons is assumed to be diagonal,  $n^{\sigma\sigma'}(\mathbf{r}) = n^\sigma(\mathbf{r})\delta_{\sigma\sigma'}$ , with the spin-up and spin-down densities  $n^\sigma(\mathbf{r})$  (for  $\sigma = \uparrow, \downarrow$  respectively) given by the equations

$$n^\sigma(\mathbf{r}) = \sum_i^N |\phi_i^\sigma(\mathbf{r})|^2 \quad (2)$$

where  $\phi_i^\sigma(\mathbf{r})$  are the single-particle eigenfunctions which solve the Kohn–Sham equations

$$\left[-\frac{1}{2}\nabla^2 + V_{eff}^\sigma(\mathbf{r})\right]\phi_i^\sigma(\mathbf{r}) = \varepsilon_i^\sigma\phi_i^\sigma(\mathbf{r}). \quad (3)$$

In these one-particle equations, the effective potential,  $V_{eff}^\sigma(\mathbf{r})$ , reads

$$V_{eff}^\sigma(\mathbf{r}) = v(\mathbf{r}) + \int \frac{n(\mathbf{r}') d\mathbf{r}'}{|\mathbf{r} - \mathbf{r}'|} + V_{xc}^\sigma(\mathbf{r}) \quad (4)$$

where  $v(\mathbf{r})$  is the ionic potential, here described as the potential due to an uniform positive charged jellium background [5], the second term on the rhs is the Coulomb–Hartree potential describing the electron–jellium interaction and  $V_{xc}^\sigma(\mathbf{r})$  is the spin-dependent exchange–correlation potential, defined as the functional derivative of the exchange and correlation energy functional,  $E_{xc}$ , with respect to the spin density  $n^\sigma$ :

$$V_{xc}^\sigma = \delta E_{xc}[n^\uparrow, n^\downarrow] / \delta n^\sigma. \quad (5)$$

Within the local-spin-density approximation (LSDA),  $E_{xc}$  reads

$$E_{xc}^{LDA}[n^\uparrow, n^\downarrow] = \int d\mathbf{r} (n^\uparrow + n^\downarrow) \varepsilon_{xc}(n^\uparrow, n^\downarrow) \quad (6)$$

where  $\varepsilon_{xc}$  is the exchange–correlation energy density per particle of the homogeneous electron system with spin densities  $n^\uparrow$  and  $n^\downarrow$ . We use for  $\varepsilon_{xc}$  the parametrization of Perdew and Wang [22]. The self-consistent solution of the LSDA Kohn–Sham equations has been successful in the calculation of spin susceptibilities in bulk alkali metals. Thus, it will we hope provide a good description of the spin modes in metal clusters, in the same way as the LDA has given a reasonable description of the plasmon states.

We discuss the response of the system to a time-dependent external field of the form  $V_{ext}^\sigma(\mathbf{r}, t) = V_{ext}^\sigma(\mathbf{r}, \omega) e^{-i\omega t}$ , which can depend on the spin component as in equation (1). This external field will induce time-dependent variations,  $\delta n^\sigma(\mathbf{r}, t)$ , in the electron spin densities. We may treat individually each Fourier component,  $\delta n^\sigma(\mathbf{r}, \omega)$ , which is defined by

$$\delta n^\sigma(\mathbf{r}, t) = \int \delta n^\sigma(\mathbf{r}, \omega) e^{-i\omega t} d\omega. \quad (7)$$

The change  $\delta n^\sigma(\mathbf{r}, \omega)$  induced in the density of electrons with spin  $\sigma$  is easily obtained from first-order time-dependent perturbation theory as:

$$\delta n^\sigma(\mathbf{r}, \omega) = \sum_{\sigma'} \int d\mathbf{r}' \chi_0^{\sigma\sigma'}(\mathbf{r}, \mathbf{r}', \omega) \delta V_{eff}^{\sigma'}(\mathbf{r}', \omega). \quad (8)$$

where  $\delta V_{eff}^{\sigma'}$  is the change induced in the effective potential

$$\delta V_{eff}^{\sigma'}(\mathbf{r}, \omega) = \delta V_{ext}^{\sigma'}(\mathbf{r}, \omega) + \sum_{\sigma'} \int d\mathbf{r}' \left[ \frac{1}{|\mathbf{r} - \mathbf{r}'|} + \frac{\delta^2 E_{xc}}{\delta n_\sigma(\mathbf{r}) \delta n_{\sigma'}(\mathbf{r}')} \right] \delta n^{\sigma'}(\mathbf{r}') \quad (9)$$

and  $\chi_0^{\sigma\sigma'}(\mathbf{r}, \mathbf{r}', \omega)$  is the response function for non-interacting electrons.

Thus, within the TDLSDA theory, the full response of the system is obtained by letting the electrons respond as free particles to an effective field which is the sum of the external one plus the induced variation of the ground state effective field.

The functions  $\chi_0^{\sigma\sigma'}$  can be expressed in terms of the eigenfunctions, eigenvalues and single-particle Green function of the LSDA ground state, as

$$\chi_0^{\sigma\sigma'}(\mathbf{r}, \mathbf{r}', \omega) = \delta_{\sigma\sigma'} \sum_{i=1}^{OCC} \left[ \phi_i^{\sigma*}(\mathbf{r}) \phi_i^\sigma(\mathbf{r}') G^\sigma(\mathbf{r}, \mathbf{r}', \varepsilon_i^\sigma + h\omega) + \phi_i^\sigma(\mathbf{r}) \phi_i^{\sigma*}(\mathbf{r}') G^\sigma(\mathbf{r}, \mathbf{r}', \varepsilon_i^\sigma + h\omega) \right] \quad (10)$$

where the Green function,  $G^\sigma(\mathbf{r}, \mathbf{r}', E^\sigma)$ , is calculated in coordinate space by solving the equation

$$[E^\sigma + \frac{1}{2}\nabla^2 - V_{eff}^\sigma(\mathbf{r}, t=0)] G^\sigma(\mathbf{r}, \mathbf{r}', E^\sigma) = \delta(\mathbf{r} - \mathbf{r}'). \quad (11)$$

By definition, the linear spin-density response function,  $\chi^{\sigma\sigma'}$ , measures the proportionality between the perturbation  $V_{ext}^{\sigma}$  and the resulting change  $\delta n^{\sigma}(\mathbf{r}, \omega)$  in the density

$$\delta n^{\sigma}(\mathbf{r}, \omega) = \sum_{\sigma'} \int d\mathbf{r}' \chi^{\sigma\sigma'}(\mathbf{r}, \mathbf{r}', \omega) V_{ext}^{\sigma'}(\mathbf{r}', \omega). \quad (12)$$

By comparing equations (8) and (12), we arrive at the following Dyson-type integral equations for the spin-density response function  $\chi^{\sigma\sigma'}(\mathbf{r}, \mathbf{r}', \omega)$  in terms of the non-interacting one  $\chi_0^{\sigma\sigma'}(\mathbf{r}, \mathbf{r}', \omega)$

$$\begin{aligned} \chi^{\sigma\sigma'}(\mathbf{r}, \mathbf{r}', \omega) &= \chi_0^{\sigma\sigma'}(\mathbf{r}, \mathbf{r}', \omega) + \sum_{\sigma_1, \sigma_2} \int d\mathbf{r}_1 d\mathbf{r}_2 \chi_0^{\sigma\sigma_1}(\mathbf{r}, \mathbf{r}_1, \omega) \left\{ \frac{1}{|\mathbf{r}_1 - \mathbf{r}_2|} + K_{xc}^{\sigma_1\sigma_2}(\mathbf{r}_1, \mathbf{r}_2) \right\} \\ &\quad \times \chi^{\sigma_2\sigma'}(\mathbf{r}_2, \mathbf{r}', \omega). \end{aligned} \quad (13)$$

In these integral equations, the kernel component,

$$K_{xc}^{\sigma\sigma'}(\mathbf{r}_1, \mathbf{r}_2) = \frac{\delta^2 E_{xc}}{\delta n^{\sigma}(\mathbf{r}_1) \delta n^{\sigma'}(\mathbf{r}_2)} \quad (14)$$

represents the residual two-body interaction due to exchange and correlation effects. The curly brackets in equation (13) contains the variation induced by the external field in the electronic terms of the Kohn–Sham effective potential, namely the spin-independent Coulomb potential and the spin-dependent exchange–correlation potential. The change induced in the ionic jellium potential is assumed to be negligible.

In a previous TDLSDA study of spin resonances specialized to unpolarized clusters responding to spin-dependent external fields, by Serra and co-workers [16], a simple response was found which can be seen as the counterpart, in the spin channel, of the dipole surface plasmon studied in [5–7]. In this paper, we have calculated, solving the integral equations (13) as matrix equations in coordinate space and developing an appropriate computational program, the response of *polarized alkali clusters* to external fields which can or cannot include the dependence on the  $z$ -component of the electronic spin (see equation (1)). This general formalism can be applied to other types of electronic system, investigating the dynamics of the electronic cloud in the dipole channel as well as in the spin channel and looking for the possible mixing between the two modes.

### 2.1. Spin-independent field

Considering an external field  $V_{ext}(\mathbf{r}, \omega)$ , which does not depend on the electron spin, the two spin electronic clouds are excited in the same way, resulting from equation (12)

$$\delta n^{\uparrow}(\mathbf{r}, \omega) = \int (\chi^{\uparrow\uparrow} + \chi^{\uparrow\downarrow}) V_{ext}(\mathbf{r}', \omega) \quad (15)$$

$$\delta n^{\downarrow}(\mathbf{r}, \omega) = \int (\chi^{\downarrow\uparrow} + \chi^{\downarrow\downarrow}) V_{ext}(\mathbf{r}', \omega). \quad (16)$$

Due to the coupling between the two spin channels, through the functions  $\chi^{\sigma\sigma'}$  of equation (13) with  $\sigma \neq \sigma'$ , the responses of the two electron clouds are not independent. This coupling is a consequence of the change in the effective correlation potential induced by the external field and it does not appear for non-interacting particles ( $\chi_0^{\sigma\sigma'} = 0$ ,  $\sigma \neq \sigma'$ ).

The theory is more easily formulated in terms of the total electron density,  $n(\mathbf{r}) = n^{\uparrow}(\mathbf{r}) + n^{\downarrow}(\mathbf{r})$ , and the spin density,  $m(\mathbf{r}) = n^{\uparrow}(\mathbf{r}) - n^{\downarrow}(\mathbf{r})$ , whose induced variations are written as

$$\delta n(\mathbf{r}, \omega) = \delta n^{\uparrow}(\mathbf{r}, \omega) + \delta n^{\downarrow}(\mathbf{r}, \omega) = \int \chi_{nn} V_{ext}(\mathbf{r}', \omega) d\mathbf{r}' \quad (17)$$

$$\delta m(\mathbf{r}, \omega) = \delta n^\uparrow(\mathbf{r}, \omega) - \delta n^\downarrow(\mathbf{r}, \omega) = \int \chi_{mn} V_{ext}(\mathbf{r}', \omega) d\mathbf{r}'. \quad (18)$$

In these equations the operators  $\chi_{nn}$  and  $\chi_{mm}$  are defined as

$$\chi_{nn} = \chi^{\uparrow\uparrow} + \chi^{\uparrow\downarrow} + \chi^{\downarrow\uparrow} + \chi^{\downarrow\downarrow} \quad (19)$$

$$\chi_{mm} = \chi^{\uparrow\uparrow} + \chi^{\uparrow\downarrow} - \chi^{\downarrow\uparrow} - \chi^{\downarrow\downarrow} \quad (20)$$

describing, respectively, the electron-density response and the spin-density response to an external potential which does not depend on the spin.

## 2.2. Spin-dependent field

Considering an external field which depends on the  $z$ -component of the electron spin,  $V_{ext}^\sigma(\mathbf{r}, \omega) = V_{ext}(\mathbf{r}, \omega)\sigma^z$ , the two spin-electronic clouds are excited in a different way. From equation (12), we have

$$\delta n^\uparrow(\mathbf{r}, \omega) = \int (\chi^{\uparrow\uparrow} - \chi^{\uparrow\downarrow}) V_{ext}(\mathbf{r}', \omega) \quad (21)$$

and

$$\delta n^\downarrow(\mathbf{r}, \omega) = \int (\chi^{\uparrow\downarrow} - \chi^{\downarrow\downarrow}) V_{ext}(\mathbf{r}', \omega) \quad (22)$$

where, as a consequence of the spin operator  $\sigma^z$ , the contributions of  $\chi^{\uparrow\downarrow}$  and  $\chi^{\downarrow\downarrow}$  to  $\delta n^\uparrow$  and  $\delta n^\downarrow$ , respectively, have the opposite sign than in equations (15) and (16). The variations in the total electron density and in the spin density are, in this case,

$$\delta n(\mathbf{r}, \omega) = \delta n^\uparrow(\mathbf{r}, \omega) + \delta n^\downarrow(\mathbf{r}, \omega) = \int_{\chi_{nm}} V_{ext}(\mathbf{r}', \omega) d\mathbf{r}' \quad (23)$$

$$\delta m(\mathbf{r}, \omega) = \delta n^\uparrow(\mathbf{r}, \omega) - \delta n^\downarrow(\mathbf{r}, \omega) = \int_{\chi_{mm}} V_{ext}(\mathbf{r}', \omega) d\mathbf{r}' \quad (24)$$

where now the operators  $\chi_{nm}$  and  $\chi_{mm}$  are defined as

$$\chi_{nm} = \chi^{\uparrow\uparrow} - \chi^{\uparrow\downarrow} + \chi^{\downarrow\uparrow} - \chi^{\downarrow\downarrow} \quad (25)$$

$$\chi_{mm} = \chi^{\uparrow\uparrow} - \chi^{\uparrow\downarrow} - \chi^{\downarrow\uparrow} + \chi^{\downarrow\downarrow} \quad (26)$$

describing, respectively, the total density response and the spin-density response to a spin-dependent external field.

For an external multipole field of the type  $V_{ext} \approx r^L Y_L(\theta, \varphi)$  with a well defined angular momentum, the corresponding responses  $R_n^L(r, \omega)$  and  $R_m^L(r, \omega)$  are given by the integrals

$$R_n^L(\omega) = \int \delta n_L(r, \omega) r^L dr \quad (27)$$

$$R_m^L(\omega) = \int \delta m_L(r, \omega) r^L dr \quad (28)$$

which represent the multipole moments with and without spin weight. The most predominant signals amongst them are the dipole,  $R_n^1$ , as well as the spin dipole,  $R_m^1$ . The imaginary part of  $R_i^1(\omega)$  ( $i = n, m$ ) is related to the strength function  $S_i^1(\omega)$  by

$$S_i^1(\omega) = \frac{1}{\pi} \text{Im} [R_i^1(\omega)]. \quad (29)$$

In the actual calculations we have artificially added an imaginary part  $\delta$  to the energy  $\omega$ . This is equivalent to convoluting the strength function with a Lorentzian, transforming the delta peaks into Lorentzians of width  $2\delta$  and thus we simplify the analysis of our results.

### 2.3. The paramagnetic case

For spin saturated clusters, our formulation reduces to the one given in [16]. In these cases we can write, after a little algebra [20]

$$K_{xc}^{\uparrow\uparrow} = K_{xc}^{\downarrow\downarrow} = K_{xc} + I_{xc} \quad (30)$$

$$K_{xc}^{\uparrow\downarrow} = K_{xc}^{\downarrow\uparrow} = K_{xc} - I_{xc} \quad (31)$$

with the operators  $K_{xc}$  and  $I_{xc}$  given by

$$K_{xc} = \frac{\delta^2 E_{xc}}{\delta n(\mathbf{r})\delta n(\mathbf{r}')} \quad (32)$$

and

$$I_{xc} = \frac{\delta^2 E_{xc}}{\delta m(\mathbf{r})\delta m(\mathbf{r}')} \quad (33)$$

respectively. In this case, the four equations (19), (20), (25), (26) reduce to

$$\chi_{nn} = \chi_{nn}^0 + \chi_{nn}^0 \left( \frac{1}{|\mathbf{r} - \mathbf{r}'|} + K_{xc} \right) \chi_{nn} \quad (34)$$

$$\chi_{mm} = \chi_{mm}^0 + \chi_{mm}^0 I_{xc} \chi_{mm} \quad (35)$$

$$\chi_{nm} = \chi_{mn} = 0 \quad (36)$$

where for free particles the correlation functions in both spin–spin and density–density responses coincide,  $\chi_{nn}^0 = \chi_{mm}^0 = \chi_0^{\uparrow\uparrow} + \chi_0^{\downarrow\downarrow}$ . Moreover, for the unpolarized case, the response of the total density to a spin-dependent field,  $\chi_{nm}$ , as well as the response of the spin density to a spin-independent external potential,  $\chi_{mn}$ , are suppressed. On the other hand, the remaining responses, that is, the total density response to a spin-independent field,  $\chi_{nn}$ , and the spin-density response to a spin-dependent field,  $\chi_{mm}$ , are not coupled one to the other. For paramagnetic systems, the spin-up and spin-down densities cancel exactly and a clean separation between the dipole and spin channels will domain the spectra.

### 3. Results and discussion

In order to illustrate the formalism developed in the previous section we apply it to jellium sodium clusters. For these systems we obtain, in this section, the response functions of the total density and of the spin density to dipole external fields with and without spin dependence.

We can imagine the excitations of the initial cluster ground state as simple spatial displacements of the electronic cloud. When the external field does not depend on the spin electron a dipole mode is generated through a shift of the whole electronic cloud with respect to the centre of the positive charge. In the case of a spin-dependent field, as in equation (1), the spin-up and the spin-down electronic densities are displaced in opposite directions such that we have an initial spin-dipole moment and a spin-dipole mode is generated.

We will check the possible cross talk between the dipole and the spin-dipole modes by calculating the spin-density response function,  $R_m$ , after a spin-independent dipole excitation as well as the total density response function,  $R_n$ , after a spin-dependent excitation. These responses are related to the operators  $\chi_{mn}$  (equation (20)) and  $\chi_{nm}$  (equation (25)), respectively. In both cases, we will draw the absolute value of the response,  $|R_i|$ , respectively, as a more robust quantity.



### 3.1. Spin-saturated clusters

As test cases we have considered the clusters  $\text{Na}_8$ ,  $\text{Na}_{20}$  and  $\text{Na}_9^+$ . They have magic electron numbers, their respective spin-up and spin-down densities are identical and their ground state shapes turn out to be spherical in the jellium model. We expect a clear separation of pure dipole modes from spin-dipole modes due to the spin symmetry. There is no response of the spin density to a spin-independent field because their variation,  $\delta m$ , is zero, and, thus, the spin mode remains asleep. There is no response either of the total density to a spin-dependent field because the centre of the whole electron cloud remains unaltered with respect to that of the positive charge. The effect of a spin-dependent field is to create a local magnetization. However, it does not induce a net magnetic moment in the whole cluster. The induced spin density,  $\delta m$ , is a spin wave, which, when spatially integrated, vanishes. Serra and co-workers [16] have observed that it is peaked at the surface allowing them to identify these modes as surface spin excitations, which have been called ‘surface paramagnons’ by analogy with the spin-wave excitations in the bulk system.

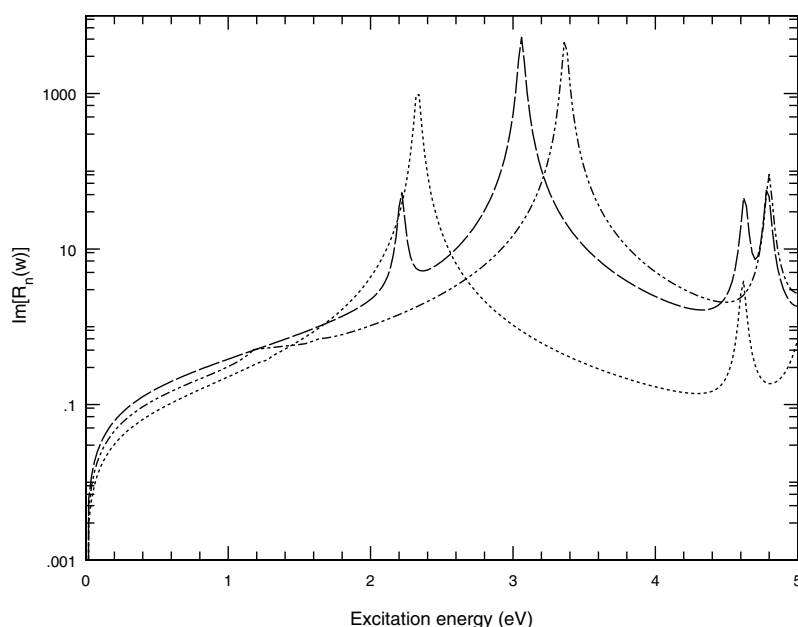


**Figure 1.** The imaginary part of the response function of the total density,  $R_n(w)$ , of  $\text{Na}_9^+$  to a dipole field, is plotted versus the excitation energy. The full response is given as the long-dashed curve. The dotted line shows the response with the  $1p \rightarrow 1d$  transition eliminated and the response with the  $1p \rightarrow 2s$  transition eliminated is plotted as the dotted-dashed line.

We discuss first the case of the  $\text{Na}_9^+$  cluster. The electronic configuration of  $\text{Na}_9^+$  in the spherical jellium model is  $1s^2 1p^6$ . The non-interacting responses to spin-independent and spin-dependent fields related to  $\chi_{nn}^0$  and  $\chi_{mm}^0$  respectively, are identical. They have simple poles at the particle-hole excitation energies, whose strength, in general, decreases for increasing energy. In the case of  $\text{Na}_9^+$  these excitations, lying at 1.56 eV and 2.18 eV, are well separated and they can be identified as the p-h transitions  $1p \rightarrow 1d$  and  $1p \rightarrow 2s$ , respectively.

When we include the induced effective potential, the resulting full responses are substantially modified. In figure 1 is shown the imaginary part of the full response function of the total density,  $R_n$ , to an external spin-independent field (long-dashed curve). Note the

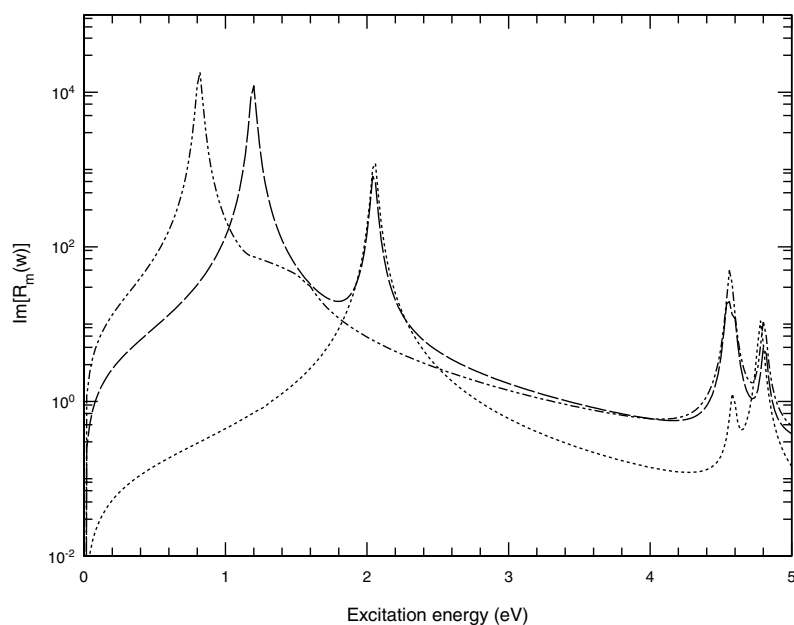


**Figure 2.** The imaginary part of the response function of the spin density,  $R_m(w)$ , of  $\text{Na}_9^+$  to a spin-dipole field, is plotted versus the excitation energy. The full response is given as the long-dashed curve. The dotted line shows the response with the  $1p \rightarrow 1d$  transition eliminated and the response with the  $1p \rightarrow 2s$  transition eliminated is plotted as the dotted-dashed line.

logarithmic scale for the strength in the figure. We can see in this dipole channel a clear and dominant peak at 3.06 eV, the well known Mie plasmon, showing the usual blue-shift with respect to the p-h excitations as a consequence of the strong and repulsive electron-electron interaction. We can analyse what leads to what in this spectrum. To analyse the composition of the plasmon peak, we have calculated the response of the system when a particular transition is suppressed in the calculation of  $\chi_{mn}^0$ . In figure 1 is also shown the full response function when the transition  $1p \rightarrow 1d$  is eliminated (dotted line spectrum), resulting in only a main peak at 2.34 eV. By eliminating the transition  $1p \rightarrow 2s$ , a resonance results at about 3.36 eV with a large strength (dotted-dashed line spectrum) and very similar to the Mie plasmon. The calculations show that the plasmon peak takes nearly all its strength from the two p-h transitions,  $1p \rightarrow 1d$  and  $1p \rightarrow 2s$ , the contribution of the first being larger, whereas the  $1p \rightarrow 2s$  transition provides the main contribution to the peak at about 2.2 eV observed in the full spectrum of figure 1.

The full response function of the spin density of  $\text{Na}_9^+$ ,  $R_m$ , to a spin-dependent field is shown in figure 2 (long-dashed curve). In this case, at variance with the response of the total density (see figure 1), the net residual interaction acting among the p-h excitations is attractive and much smaller than in the dipole channel. The Hartree contribution leads to cancelling oscillations of up and down electronic clouds, and the remaining induced potential is due to the exchange and correlation contribution, which is attractive. As a main consequence, the strength shifts to lower energies than the p-h transitions and leads to essentially one peak at 1.2 eV, which we identify as a collective spin excitation, which exhausts a large fraction of the spin-dipole sum rule. This state washes out, almost completely, the low-energy p-h transitions. In figure 2 are also shown the response functions when the transitions  $1p \rightarrow 1d$

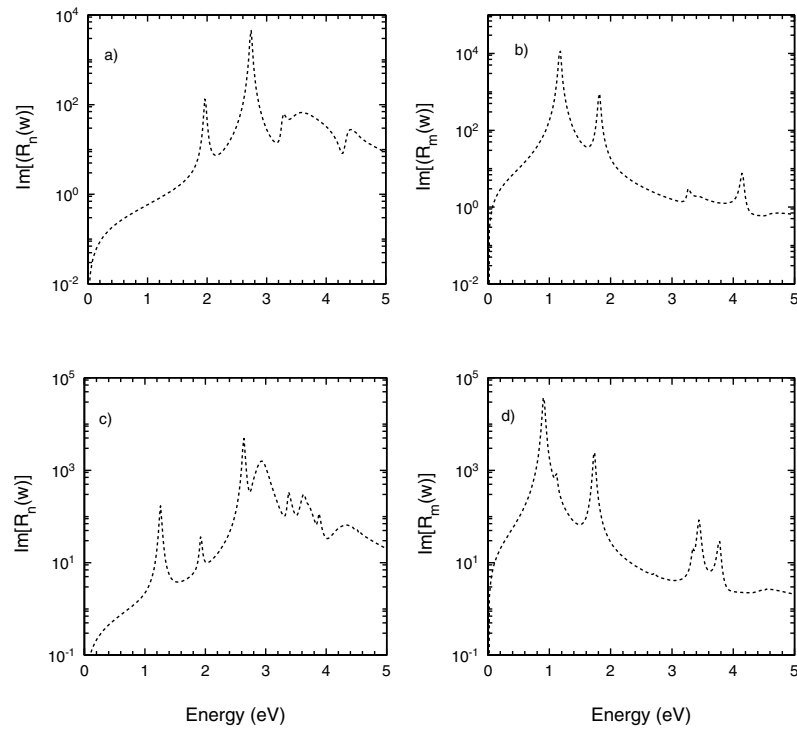


**Figure 3.** The imaginary part of the response functions of  $\text{Na}_8$  and  $\text{Na}_{20}$  clusters is plotted versus the excitation energy. (a) The full response,  $R_n$ , of  $\text{Na}_8$  to a dipole field; (b) the full response,  $R_m$ , of  $\text{Na}_8$  to a spin-dipole field; (c) the full response,  $R_n$ , of  $\text{Na}_{20}$  to a dipole field; (d) the full response,  $R_m$ , of  $\text{Na}_{20}$  to a spin-dipole field.

(dotted line) and  $1p \rightarrow 2s$  (dotted-dashed line) are eliminated. In the first case, a peak appears at 2.16 eV and in the second case there is a main resonance at 0.82 eV similar to the spin mode. Superimposing these two profiles, we obtain a spectrum similar to the full response, but shifted to lower energies. The contribution of the transition  $1p \rightarrow 1d$  to the strength of the spin mode is larger, as in the case of the Mie plasmon dipole mode of figure 1. The higher-lying p-h transitions are not so strongly affected by the interaction. They are only slightly shifted in energy, still keeping approximately their original strength.

In the case of an external mixed excitation, which includes spin and no-spin components,  $V_{ext}^\sigma = \sum_{j=1}^N r_j^L Y_{L0}(1 + \sigma_j^z)$ , the dipole and spin-dipole channels will be excited with comparable strength. The two different channels will develop independently and the resulting spectrum will be the linear superposition of the spectra shown in figures 1 and 2.

For the sake of completeness we present in figure 3 the response functions of the total density and of the spin density of  $\text{Na}_8$  and  $\text{Na}_{20}$  clusters.

The non-interacting response of  $\text{Na}_8$  has two peaks at 1.5 eV and 1.92 eV, due to the transitions  $1p \rightarrow 1d$  and  $1p \rightarrow 2s$ , respectively. The full response functions of  $\text{Na}_8$  to dipole excitation and to spin-dipole excitation are respectively represented in figures 3(a) and 3(b). As in the case of  $\text{Na}_8^+$ , a perfect separation of the modes can be observed. The Mie plasmon resonance appears at 2.74 eV in the dipole channel, together with another peak at lower energy (1.98 eV) and with smaller strength. There is some structure at around 4 eV corresponding to a mix of p-h states sitting near the ionization threshold. Photo-depletion experiments [23]

show a main resonance at 2.53 eV with a width of 0.19 eV for this cluster. A better theoretical description of the ionic background leads to a TDLDA resonance at 2.55 eV [4, 24, 25], very close to the experimental value. The spin mode of  $\text{Na}_8$  appears, in figure 3(b), as a pronounced peak at 1.16 eV very close to the first p–h excitations. This result agrees with the previous calculations by Serra and co-workers [16], although obtained with a slightly different density functional.

The  $\text{Na}_{20}$  cluster has the ground state electronic configuration  $1s^2 1p^6 1d^{10} 2s^2$  in the jellium model. For the non-interacting response there are several low-energy transitions that lie very close. The strength function,  $R_n$ , for a dipole excitation shows (figure 3(c)) a multi-peaked structure with two main resonances lying at 2.64 eV and at 2.94 eV, somewhat below the threshold for electron detachment. Quantum size effects leading to the breaking of the strength (Landau fragmentation) are quite clear in this spectrum and already they have been extensively discussed at the level of TDLDA. The fragmentation is due to the coupling between the surface plasmon and discrete, bound, electron–hole excitations which occur at an excitation energy nearly degenerate with the plasmon energy. The measured photoabsorption cross section for  $\text{Na}_{20}$  [23] shows two main transitions at 2.42 eV and 2.78 eV (widths of 0.2 eV and 0.4 eV, respectively). The calculated response function,  $R_m$ , of  $\text{Na}_{20}$  to the spin-dependent field (figure 3(d)) shows a broad and strong resonance at 0.9 eV (spin mode) and another smaller resonance at 1.7 eV.

Comparing the  $\text{Na}_8$  and  $\text{Na}_{20}$  spectra we can infer the evolution of the spin modes with the cluster size. The short-range interaction causes the energy of the collective state to decrease with increasing size following the trend  $\propto N^{-1/3}$ , in a way that resembles the behaviour of the analogous nuclear collective excitations, and that is opposite to that exhibited by the Mie plasmons. For increasing sizes, the residual interaction is less and less effective in separating the collective spin state from the p–h excitations. Thus, for large clusters, we expect to approach the bulk picture in which the spin wave excitations are strongly damped by surrounding p–h excitations (Landau damping).

### 3.2. Clusters with open shells

There are several examples of clusters where spontaneous spin polarization occurs in the ground state or in a low-lying isomer [26]. In this section we study the response of selected spin-polarized clusters, the spherical isomer of  $\text{Na}_6^+$  and the  $\text{Na}_{13}$  sodium cluster. We expect a natural mixing of the dipole and the spin-dipole modes in the responses of the total density as well as of the spin density to external fields. The global motion of the whole electronic cloud will excite the spin mode and, conversely, the displacements of the up and down spin densities into opposite directions will excite also the dipole mode.

The  $\text{Na}_6^+$  cluster is triaxial in its background state [26, 27], but we consider instead the isomeric spherical state of  $\text{Na}_6^+$  which is strongly spin polarized [26]. This isomer is an example where spontaneous spin polarization occurs in the ground state, leading to the electronic configuration  $1s^2 1p^3$ , with the three p electrons having the same spin component. In this state we can study the cross talk between the dipole and the spin-dipole channels without bothering about additional features due to structural degrees of freedom.

The main allowed p–h transitions are  $1s^\downarrow \rightarrow 1p^\downarrow$  at 1.64 eV,  $1p^\uparrow \rightarrow 1d^\uparrow$  at 1.94 eV and  $1p^\uparrow \rightarrow 2s^\uparrow$  at 2.50 eV. The first one, which is not possible for closed-shell clusters ( $\text{Na}_9^+$ ,  $\text{Na}_8$  and  $\text{Na}_{20}$ ), originates from the main qualitative differences between the screened responses of these clusters and those of the  $\text{Na}_6^+$  cluster. The calculated strength function,  $R_n$ , for the dipole excitation, is shown in figure 4(a). We can see the usual pattern of the Mie plasmon response, caused by a strongly repulsive residual interaction, which shifts the plasmon to 3.18 eV, a

much higher energy than the unperturbed p–h transitions. In figure 4(b) the response function,  $R_m$ , resulting from a spin-dipole excitation, is also shown. It is visible that the strength is red-shifted with respect to the relevant p–h transitions, due to the attractive residual interaction in the spin channel, the spin mode appearing at 1.38 eV.

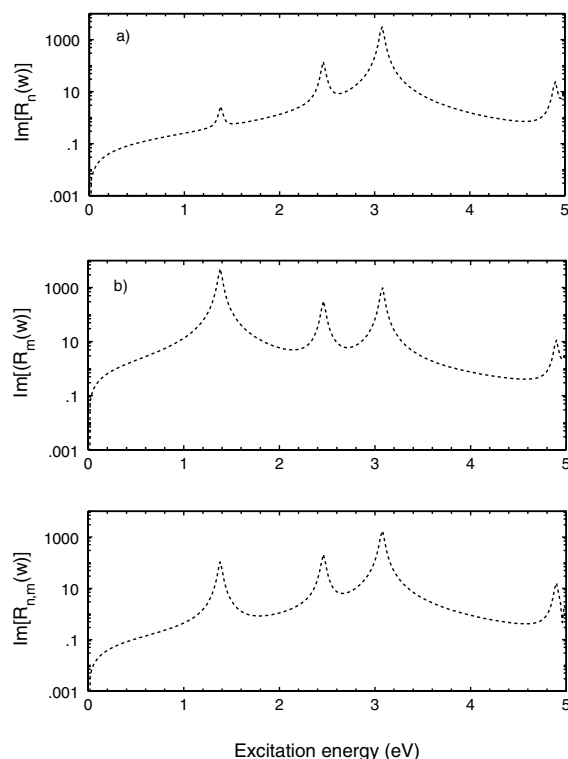


**Figure 4.** The imaginary part of the response functions of  $\text{Na}_6^+$  is plotted versus the excitation energy. (a) The full response of the total density to a dipole field; (b) the full response of the spin density to a spin-dipole field; (c) the full response of the total density (spin density) to a spin-dipole field (dipole field).

It is interesting to note that the positions of the spin mode and of the plasmon mode are nearly the same as for  $\text{Na}_9^+$ . It is a general feature of these collective modes that they depend only weakly on the size of the system.

The main qualitative difference between these spectra and those of spin-saturated clusters is that the spin polarization of the  $\text{Na}_6^+$  cluster mixes dipole and spin-dipole modes very efficiently. Both channels interact each one with the other, that is, a signal in the dipole (spin-dipole) mode is visible in the spin-dipole (dipole) spectrum at 3.08 eV (1.38 eV), as can be seen in figures 4(a) and 4(b). This fact will overlay the p–h transitions at low energies by the spin mode, and thus it will be hard to distinguish the p–h modes experimentally, when a spin-independent field is applied, unless one can ascertain independently that one deals with an even cluster having no spontaneous spin polarization.

Moreover, each perturbation, dipole as well as spin dipole, excites both channels with comparable strength. Thus, figure 4(c) shows the full response function of the density response to a spin-dipole excitation, which coincides in the case of half-filled shell clusters such as  $\text{Na}_6^+$  with the strength function of the spin-density response for a dipole excitation. Now, these

responses are not suppressed as in the case of unpolarized clusters and significant cross talk between dipole and spin-dipole modes are detected from this figure, where one can see a small copy of the spin mode and a response in the region of the dipole plasmon.

On the other hand, it is interesting to note that the positions of the peaks of the three figures 4 are the same. The difference is the relative strength of each mode. Each excitation type prefers its related mode.

As in the case of the spin-saturated cluster,  $\text{Na}_9^+$ , the plasmon peak and the spin-dipole mode take their strength from the  $1p^\uparrow \rightarrow 1d^\uparrow$  and  $1p^\uparrow \rightarrow 2s^\uparrow$  p-h transitions. The response functions  $R_n$  and  $R_m$ , when the  $1p^\uparrow \rightarrow 1d^\uparrow$  transition is eliminated, to spin-independent and spin-dependent fields, are respectively shown in figures 5(a) and 5(d). In this case, neither the dipole nor the spin-dipole modes appear. In figures 5(b) and 5(e) are respectively shown the dipole and the spin-dipole spectra when the  $1p^\uparrow \rightarrow 2s^\uparrow$  transition is suppressed. The additional peak shown in all previous full responses, at about 2 eV, does not appear in any of these spectra. However, the plasmon and the spin mode turn out to be shifted with respect to their original positions in the full spectra, as in the case of closed-shell clusters. There is another peak due to the down p-h transition  $1s^\downarrow \rightarrow 1p^\downarrow$ . This p-h transition is the origin of the interaction between the two channels, dipole and spin dipole, and when it is eliminated the dipole spectrum looks like the full spectrum of  $\text{Na}_6^+$  (see figure 5(c)). The two resonances, which were obtained in the case of this cluster, result now at 2.82 eV and 2.44 eV. The most important fact is that the 'spin-mode signal' does not appear. We can conclude that the  $1s^\downarrow \rightarrow 1p^\downarrow$  down-transition causes the correspondence between the resonances observed in the full dipole and spin-dipole spectra and the cross talk between the two modes.

Another cluster with spin-polarized configuration is  $\text{Na}_{13}$ . This cluster has the ground state electronic configuration  $1s^2 1p^6 1d^5$  in the spherical jellium model. The more relevant p-h transitions are  $1d^\uparrow \rightarrow 1f^\uparrow$ ,  $1p^\downarrow \rightarrow 1d^\downarrow$ ,  $1d^\uparrow \rightarrow 2p^\uparrow$ ,  $1p^\downarrow \rightarrow 2s^\downarrow$  and  $1p^\downarrow \rightarrow 2s^\downarrow$ , lying respectively at 1.38 eV, at 1.43 eV, at 1.50 eV, at 1.54 eV and at 1.71 eV. The full response of the total density to a pure dipole field shows a broad resonance at 2.88 eV, which corresponds to the Mie plasmon. On the other hand, when we calculate the full response of the spin density to a spin-dipole perturbation, the collective spin mode is obtained at 1.1 eV. The response of the total density to a spin-dipole external field and the one of the spin density to a pure dipole field are identical, in the same way as the  $\text{Na}_6^+$  cluster. In figure 6 we represent all these spectra. From the analysis of these spectra, we obtain conclusions analogous to those in the previous case.

#### 4. Summary and conclusions

We have investigated the response of the electronic cloud of spin-saturated and spin-polarized metal clusters to dipole as well as spin-dipole perturbations in the linear regime within the TDLSDA method of density functional theory. We generalize the TDLSDA approach of Serra and co-workers [16], which was applied only to closed-shell alkali clusters. Thus, we have analysed the cross talk between dipole and spin-dipole modes. As test cases, we have studied the spin-saturated clusters  $\text{Na}_9^+$ ,  $\text{Na}_8$  and  $\text{Na}_{20}$ , and the strongly spin-polarized clusters  $\text{Na}_6^+$  and  $\text{Na}_{13}$ .

In all these cases we obtain a dominant Mie plasmon resonance in the optical region when a spin-independent field is applied. Under the influence of a spin-dependent field the system develops another strongly collective mode that lies in the low-energy part of the spectrum (about 1 eV), that is, at energies below the corresponding p-h transitions, as a consequence of the attractive residual interaction. This spin mode, which decreases for increasing sizes, corresponds to oscillations of spin-up electrons against spin-down electrons and may be

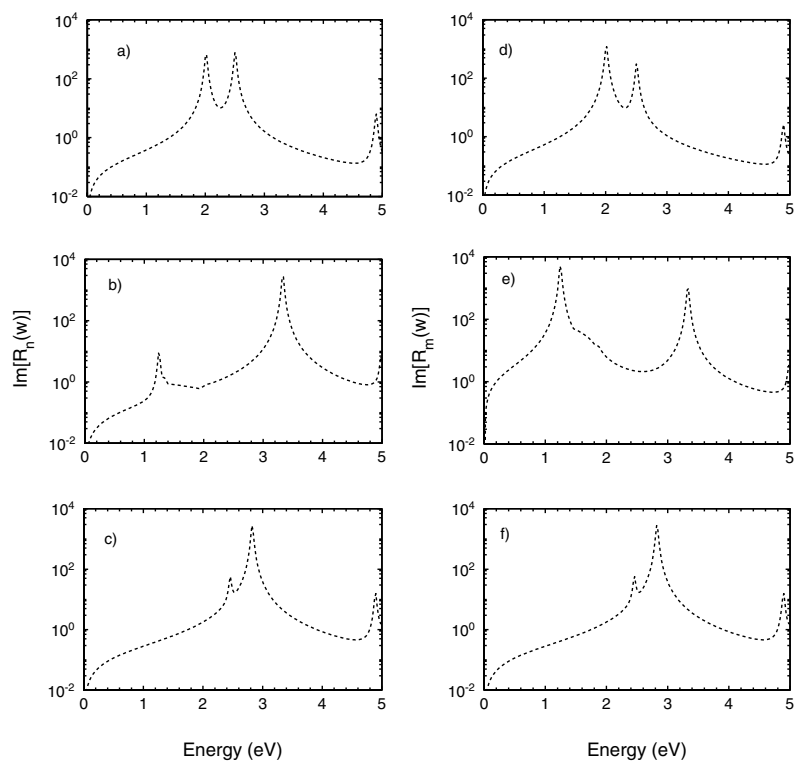


**Figure 5.** The imaginary part of the response functions of  $\text{Na}_6^+$ , when some transitions are suppressed, is plotted versus the excitation energy. (a) The response,  $R_n$ , with the  $1p^\uparrow \rightarrow 1d^\uparrow$  transition eliminated. (b) The response,  $R_n$ , with the  $1p^\uparrow \rightarrow 2s^\uparrow$  transition eliminated. (c) The response,  $R_n$ , with the  $1s^\downarrow \rightarrow 1p^\downarrow$  transition eliminated. (d) The response,  $R_m$ , with the  $1p^\uparrow \rightarrow 1d^\uparrow$  transition eliminated. (e) The response,  $R_m$ , with the  $1p^\uparrow \rightarrow 2s^\uparrow$  transition eliminated. (f) The response,  $R_m$ , with the  $1s^\downarrow \rightarrow 1p^\downarrow$  transition eliminated.

regarded as the counterpart, in the spin channel, of the dipole surface plasmon, appearing in the dipole channel.

Both modes, dipole and spin dipole, are well separated in the case of spin-saturated clusters, but they intertwine for spin-polarized clusters, independently of the spin dependence or spin independence of the external fields. This happens because a global motion of the whole electron cloud inevitably excites always the spin mode, because up and down densities are different. This cross talk means that a real chance exists to observe the spin modes by optical absorption, at least indirectly.

The main difference in the non-interacting response between spin-saturated and spin-polarized clusters is the existence of p-h transitions from occupied spin-down to unoccupied spin-down levels for the latter clusters, which are responsible for the mixing between the modes.

While the jellium model is presumably sufficient for exhibiting qualitative trends, access to details at spectroscopic accuracy requires a full account of the ionic structure. Taking into account a detailed ionic background produces a splitting of the plasmon into different frequencies. This collective splitting is one of the basic features of the dipole plasmon which was noted very early [5] and which has been exploited extensively to explore the cluster geometry from analysing optical response. We expect also a fragmentation of the spin-dipole

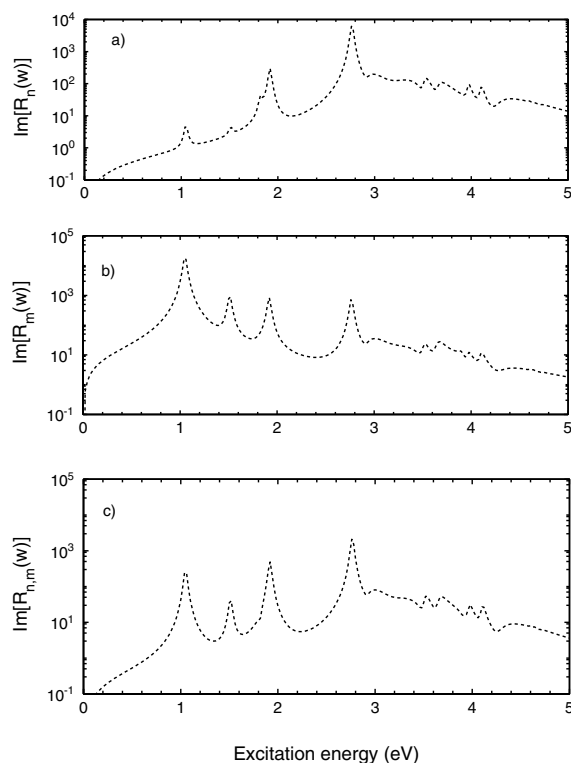


**Figure 6.** The imaginary part of the response functions of  $\text{Na}_{13}$  is plotted versus the excitation energy. (a) The full response of the total density to a dipole field. (b) The full response of the spin density to a spin-dipole field. (c) The full response of the total density (spin density) to a spin-dipole field (dipole field).

spectra [12] in the same way, negligible for the unpolarized ground state but large for the polarized clusters. But, the coupling between dipole and spin-dipole modes that we have studied here will remain as a basic feature, and moreover, the splitting effect will be smaller for large clusters where the electronic fluctuations seem to dominate the spatial structure.

The general TDLSDA method here presented provides a useful way to study the response of pure alkali clusters as well as the response of other systems, as could be the case of doped clusters with an atom at the centre. In the near future, we will show calculations on the spin-dipole response of sodium clusters with a lead atom, whose ground state properties have been recently studied by the second author [28].

On the other hand, the first results about the spin modes obtained using the hydrodynamic model by Lipparini and Califano [15] have assumed the equilibrium density of the valence electrons to be a constant that has the bulk value. This fact neglects the surface effect associated with the spill-out of the electrons outside the jellium edge, particularly important in small clusters. This effect is mainly responsible for the differences between the predictions of the hydrodynamic approach and those of the TDLSDA calculations for the frequencies of the collective modes. In the future, we can investigate the diffusibility of the valence electrons on the spin modes starting from the hydrodynamic method and compare with our TDLSDA results, as in a recent paper of Providencia and the first author [29] about dipole modes.



## Acknowledgments

This work has been supported by DGICYT (grant No PB95-0202) and Junta de Castilla y León (grant No VA70/99).

## References

- [1] de Heer W 1993 *Rev. Mod. Phys.* **65** 611
- [2] Brack M 1993 *Rev. Mod. Phys.* **65** 677
- [3] de Heer W A *et al* 1987 *Phys. Rev. Lett.* **59** 1805  
Selby K 1989 *Phys. Rev. B* **40** 5417  
Brechignac C *et al* 1989 *Chem. Phys. Lett.* **164** 433  
Brechignac C *et al* 1989 *Phys. Rev. Lett.* **63** 1368  
Reiners T *et al* 1995 *Phys. Rev. Lett.* **74** 1558  
Ellert C *et al* 1995 *Phys. Rev. Lett.* **75** 1731  
Reiners T *et al* 1993 *Chem. Phys. Lett.* **215** 357  
Ellert C *et al* 1995 *Phys. Rev. Lett.* **75** 1731  
Borggreen J *et al* 1995 *Phys. Rev. B* **48** 17507
- [4] Rubio A *et al* 1996 *Phys. Rev. Lett.* **77** 247 and references therein
- [5] Ekardt W 1984 *Phys. Rev. Lett.* **52** 1925  
Ekardt W 1985 *Phys. Rev. B* **31** 6360  
Beck D E 1991 *Phys. Rev. B* **35** 7325
- [6] Zangwill A and Soven P 1980 *Phys. Rev. A* **21** 1561
- [7] Yannouleas C *et al* 1989 *Phys. Rev. Lett.* **63** 255  
Yannouleas C *et al* 1990 *Phys. Rev. B* **41** 6088  
Yannouleas C and Broglia R A 1991 *Phys. Rev. A* **44** 5793
- [8] Kummel S, Brack M and Reinhard P-G 1998 *Phys. Rev. B* **58** R1774
- [9] Yabana K and Bertsch G F 1999 preprint physics/9903041
- [10] Yabana K and Bertsch G F 1998 *Phys. Rev. A* **58** 2604
- [11] Calvayrac F, Reinhard P-G and Suraud E 1998 *J. Phys. B: At. Mol. Phys.* **31** 1367
- [12] Kohl C, El-Gammal S M, Calvayrac F, Suraud E and Reinhard P-G 1999 *Eur. Phys. J.* **5** 271
- [13] Sham L J 1965 *Proc. R. Soc. A* **283** 33  
Woods A D B *et al* 1962 *Phys. Rev.* **128** 1112
- [14] Richter A 1979 *Nuclear Physics with Electromagnetic Interactions. Proc. (Mainz, 1979)* Arenhovel H 1979, *Lecture Notes in Physics* vol 108, (Berlin: Springer) p 19
- [15] Lipparini E and Califano M 1996 *Z. Phys. D* **37** 365  
Serra LI and Lipparini E 1997 *Z. Phys. D* **42** 227
- [16] Serra LI, Broglia R-A, Barranco M and Navarro J 1993 *Phys. Rev. A* **47** R1601
- [17] Mornas L, Calvayrac F, Suraud E and Reinhard P-G 1996 *Z. Phys. D* **38** 73
- [18] Calvayrac F *et al* 1995 *Phys. Rev. B* **52** 17056
- [19] Williams A R and Von Barth U 1983 *Theory of the Inhomogeneous Electron Gas* ed S Lundqvist and N H March (New York: Plenum). See also Liu K L and Vosko S H 1989 *Can. J. Phys.* **67** 1015
- [20] Torres M B 1997 *PhD Thesis* Valladolid University
- [21] Van Ruitenbeek J M 1991 *Z. Phys. D* **19** 247
- [22] Perdew J-P and Wang Y 1992 *Phys. Rev. B* **45** 13244
- [23] Wang C R C *et al* 1990 *Chem. Phys. Lett.* **166** 26  
Wang C R C *et al* 1991 *J. Chem. Phys.* **94** 2496  
Wang C R C *et al* 1990 *J. Chem. Phys.* **93** 3787  
Wang C R C *et al* 1991 *Z. Phys. D* **19** 13  
Selby K, Kresin V, Masui J, Vollmer M, de Heer W-A, Scheidemann A and Knight W 1991 *Phys. Rev. B* **43** 4565
- [24] Bonacić-Koutecky V *et al* 1990 *J. Chem. Phys.* **93** 3802  
Gatti C *et al* 1990 *Chem. Phys. Lett.* **175** 645
- [25] Andreoni W 1989 *Progress on Electron Properties of Solids* (Dordrecht: Kluwer)
- [26] Kohl C, Montag B and Reinhard P-G 1995 *Z. Phys. D* **35** 57
- [27] Karspel S, Kohl C and Reinhard P-G 1995 *Phys. Lett. A* **206** 81
- [28] Balbás L C and Martins J L 1996 *Phys. Rev. B* **54** 2937
- [29] da Providencia J Jr and Torres M B 1999 *J. Phys.: Condens. Matter* **11** 8459